Generation and Characterization of New Fluoro-Substituted Carbenes

Christophe Buron, Eric M. Tippmann, and Matthew S. Platz*

Department of Chemistry, The Ohio State University, 1118 Newman-Wolfrom, 100 West 18th Avenue, Columbus, Ohio 43210

Received: August 11, 2003; In Final Form: December 1, 2003

Singlet fluorocarbenes substituted with diphenylphosphanyl, phenylsulfanyl, and trimethylsilyl groups were generated upon photolysis of the corresponding tricyclo[4.3.1.0]decadiene precursors **1a**−**c**. Diphenylphosphanyl fluoro carbene **2a** was directly observed by transient UV−Vis spectroscopy. Its lifetime in several solvents ranged from 1 to 10 μs. A study of its reactivity toward methyl acrylate and tetramethylethylene along with DFT calculations did not indicate specific solvation of the carbene center. Fluorothiophenyl carbene **2b** and fluorotrimethylsilyl carbene **2c** were studied by their reaction with pyridine to form ylides and have lifetimes of 1 μs (cyclohexane) and 33 ns (carbon tetrachloride), respectively, at room temperature. Transient UV−Vis spectroscopy supported by DFT calculations showed that, in the case of fluorothiophenyl carbene **2b**, carbene formation is in competition with the generation of the diradical intermediate formed by the cleavage of only a single C−C bond of the cyclopropane ring of the precursor.

I. Introduction

Vogel-Jones type precursors (e.g., **1**) have proven to be useful photochemically activated sources of halocarbenes **2** (Scheme 1).[1] This type of precursor can often be more convenient than the more common diazirine and diazo precursors for certain carbenes.[2] Herein, we report the preparation of three new precursors, **1a**−**c**, studies of their photochemistry, and kinetic spectroscopy of related carbenes **2a**−**c**. This permits the first generation and characterization of fluorocarbenes substituted with phosphorus, sulfur, and silicon.

II. Experimental Section

Synthesis. Dihydroindan **4** was prepared by Birch Reduction of indan **3** as described in the literature.[3] All chemical reagents were used as purchased from Sigma Aldrich. All reaction solvents were distilled under a dry argon atmosphere. THF was distilled over sodium and benzophenone, diisopropylamine over calcium hydride, and triethylamine over potassium hydroxide. NMR spectra were recorded using a Brucker DPX-250 or DPX-400 MHz spectrometers as noted. Chemical shifts are reported positively downfield and are expressed in ppm relative to triethylsilane (^{1}H and ^{13}C), CF_3COOH (^{19}F), or 10% H_3PO_4 (^{31}P).

10-Chloro-10′-fluorotricyclo[4.3.1.0^{1,6}]deca-3-ene (5). A procedure of Dolbier and Burkholder was followed closely.[4] To a 1L RBF fitted with a mechanical stirrer and condenser was added 600 mL of dry THF. The flask was cooled to 0 °C, and 50 mL of $TiCl_4$ was added dropwise, under an argon atmosphere, over 1 h. HCl gas was evolved and the flask was open to the atmosphere to prevent pressure buildup. The reaction mixture turned bright yellow. $LiAlH_4$ (17.26 g) was added as a powder to the reaction in 2.5 g portions over 45 min. Gas was evolved and the flask was vented to the atmosphere. The reaction mixture turned dark brown. The reaction was allowed to warm to RT and was stirred 30 min. The reaction was cooled to 0 °C, and dihydroindan **4** (21.5 mL) was added slowly. Using a syringe pump, a solution of 19 mL of $CFCl_3$ in 60 mL of THF was added to the reaction over 2 h. The reaction was stirred an additional 1 h then poured into 400 mL of cold aqueous 10% HCl. The acidic aqueous solution was extracted with ether (2

SCHEME 1

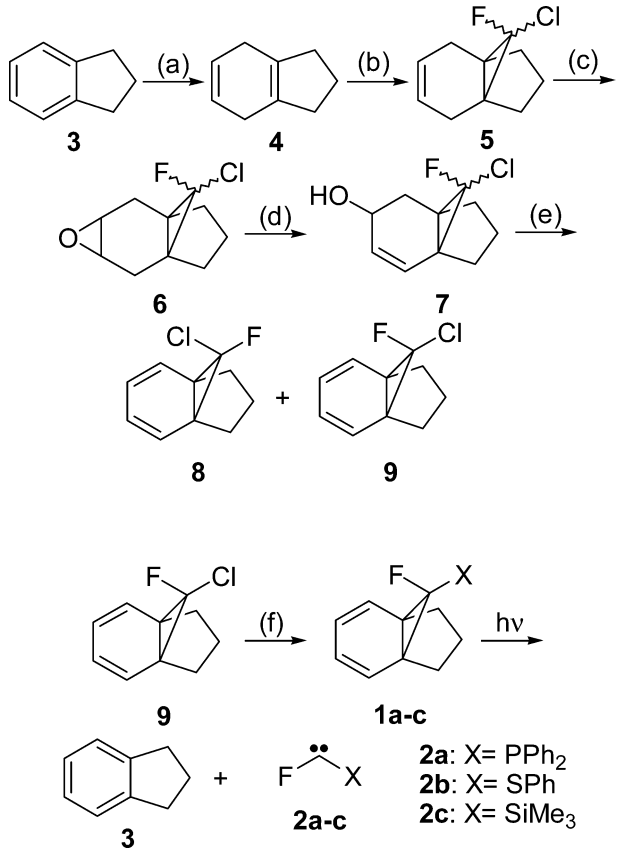

(a) (i) $Na_{(s)}/NH_{3(l)}$ −50 °C (ii) MeOH; (b) (i)$TiCl_4/LiAlH_4$, 2 eq. (ii) $CFCl_3$ 1.1 eq. 0 °C THF; (c) MCPBA, CH_2Cl_2, RT; (d) (i) diisopropylamine/*n*-BuLi 3 eq. (ii) H_2O 0 °C THF; (e) (i) 3.5 eq. NEt_3 (ii) 3.5 eq. MsCl 0 °C THF; (f) (i) *n*-BuLi, −78 °C (ii) electrophile (X^+).

* Corresponding author. E-mail: Platz.1@osu.edu.

10.1021/jp0363848 CCC: $27.50 © 2004 American Chemical Society
Published on Web 01/15/2004

× 500 mL) and CH_2Cl_2 (1 × 500 mL). The combined organic phase was washed with 20% $NaHCO_3$ (1 × 150 mL). The solution was dried over $MgSO_4$, filtered, and then the solvent was removed by rotary evaporation to yield a red-brown oil. The product was passed over silica gel with pentane elution to yield 29.5 g (90%) of clear oil of the two isomers and a small amount of starting material. ^{19}F NMR (235 MHz, $CDCl_3$): δ −139.1 (s, 1F); −146.5 (s, 1F). ^{1}H NMR (400 MHz, $CDCl_3$): δ 1.6−2.7 (m, 20H); 5.81 (s, 2H); 5.86 (s, 2H). ^{13}C NMR (101 MHz, $CDCl_3$): δ 24.3; 24.4; 24.6; 24.9; 25.6; 25.7; 33.3; 34.1; 34.2; 36.0; 36.1; 36.2; 123.2; 123.3; 124.7; 126.9. MS (EI) *m*/*z* 186 (5%); 151 [−Cl] (100%).

10-Chloro-10′-fluorotricyclo[4.3.1.0^{1,6}]deca-3-oxirane (6). To a round-bottom flask containing 225 mL of CH_2Cl_2 cooled in an ice bath was added 29.5 g of alkene **(5)** followed by 35.5 g of solid *m*-chloroperoxybenzoic acid (MCPBA) in four portions, with magnetic stirring. After the last portion of MCPBA was added, the reaction was brought to room temperature and stirred 2 h. The reaction was cooled to −20 °C, and the benzoic acid was removed by filtration. Unreacted MCPBA was removed by washing with 10% aqueous sodium bisulfite. The filtrate was then washed with 10% sodium carbonate, dried with $MgSO_4$, filtered, and rotavapped to yield a clear oil. The crude product was passed over silica gel with hexane elution to remove all nonpolar impurities followed by 1:20 ether/hexanes to elute the product. The appropriate fractions were collected and concentrated for a 94% yield of two isomers. ^{19}F NMR (235 MHz, $CDCl_3$): δ −133.7 (s, 1F); −148.1 (s, 1F). ^{1}H NMR (400 MHz, $CDCl_3$): δ 1.5−1.7 (m, 8H); 1.8−2.3 (m, 12H); 3.06 (d, 4H, J = 6.0 Hz). ^{13}C NMR (101 MHz, $CDCl_3$): δ 20.9; 21.0; 23.0; 23.4; 29.2; 24.4; 31.9; 32.2; 32.3; 36.4; 36.5; 50.2; 50.3; 50.4. MS (EI) *m*/*z* 202 (2%), 167 [−Cl] (56%), 146 [−F] (100%).

10-Chloro-10′-fluorotricyclo[4.3.1.0^{1,6}]deca-4-ene-2-ol (7). To a flame-dried RBF was introduced 50 mL of dry THF. This was followed by the addition of 26 mL of diisopropylamine. The flask was cooled to −5 °C, then 116 mL of *n*-BuLi (1.6 M in hexanes) was added dropwise over 30 min and stirred 25 min. The starting epoxide **(6**, 10 g, 0.187 mol) was dissolved in 25 mL of dry THF and added to the reaction over 1 h via syringe pump. The reaction became increasingly reddish during the addition and was stirred for 2 h. The reaction was quenched with the dropwise addition of 25 mL of water, and then poured into 700 mL of ice water. The reaction was neutralized by adding 10% aqueous HCl. The aqueous phase was extracted with CH_2Cl_2 (2 × 300 mL). The combined organic phase was washed with water (2 × 250 mL), dried ($MgSO_4$), filtered, and concentrated to yield 18 g of a crude reddish oil. Chromatography (silica gel, CH_2Cl_2 elution) yielded 10.6 g of a clear oil (82% yield) of isomers. Further purification can be achieved by chromatography a second time on silica with a 10:90 mixture of ether/hexanes followed by elution with 30:70 ether/hexanes. ^{19}F NMR (235 MHz, $CDCl_3$): δ −132.3 (s, 1F); −139.2 (s, 1F). ^{1}H NMR (400 MHz, $CDCl_3$): δ 1.69−1.71 (m, 2H); 1.84−1.95 (m, 4H); 2.0−2.2 (m, 8H); 2.48 (q, J = 7.8 Hz); 2.56 (q, J = 7.8 Hz); 4.18 (m, 1H); 4.29 (m, 1H); 5.79 (dd, J = 2.3 Hz, J = 3.8 Hz); 5.85 (m); 6.0 (d, J = 10.0 Hz). ^{13}C NMR (101 MHz, $CDCl_3$): δ 26.0; 26.1; 26.3; 26.4; 30.9; 31.9; 32.1; 32.6; 35.4; 37.7; 36.8; 36.9; 38.3; 38.4; 64.1; 65.0; 123.9; 124.0; 127.3; 131.8; 132.5.

10-Chloro-10′-*exo*-fluorotricyclo[4.3.1.0^{1,6}]deca-2,4-diene (8) and 10-*exo*-Chloro-10′-fluorotricyclo[4.3.1.0^{1,6}]deca-2,4-diene (9). The alcohol **7** (20 g), was dissolved in 75 mL of CH_2Cl_2. A quantity of 17.5 mL of triethylamine was added at 0 °C followed by dropwise addition of 10 mL of methane sulfonyl chloride. The reaction was stirred overnight at 0 °C to RT and a white solid precipitated. The reaction was poured into 150 mL of ice water and separated. The organic layers were washed with 2 M HCl (1 × 75 mL) and then the aqueous phase was extracted with CH_2Cl_2 (2 × 75 mL). The organic phase was dried over $MgSO_4$, filtered, and concentrated by rotary evaporation to yield 10.5 g of a reddish-orange mixture. Chromatography (silica gel, hexanes elution) afforded 8.5 g of a mixture of isomers (75%) as a clear oil. A more stringent separation was able to completely separate the isomers but typically the subsequent reactions were performed with the isomeric mixture. ^{19}F NMR (235 MHz, $CDCl_3$): δ −130.2 (s, 1F), −164.9 (s, 1F). ^{1}H NMR (400 MHz, $CDCl_3$): δ 1.6−1.8 (m, 2H); 1.9−2.1 (m, 2H); 2.3−2.5 (m, 2H); 5.86 (m, 2H); 6.05−6.13 (m, 2H). ^{13}C NMR (101 MHz, $CDCl_3$): δ 123.5 (d, J = 1.1 Hz); 119.5 (d, J = 9.4 Hz); 102.6 (d, J = 412 Hz); 50.7 (d, J = 11.1 Hz); 34.8 (s); 26.2 (d, J = 2.2 Hz). MS (EI) *m*/*z* 183 (2.5%), 149 [−Cl] (100%).

Synthesis of Compounds 1a−c. General Procedure. A mixture of compounds **8** and **9** under an inert atmosphere of argon was dissolved in dry THF and cooled to −78 °C. The relative ratio of **8**:**9** was determined by either ^{19}F NMR or GC/MS. Then 1.1 equivalents (relative to **8**) of *n*-butyllithium in hexanes were added in one portion. The mixture was stirred at low temperature for 2 h. Then 1 equivalent of electrophile was introduced (e.g., chlorodiphenylphosphine, benzenesulfanyl chloride, or chlorotrimethylsilane). The cold bath was removed and the solution was allowed to warm to room temperature. THF was evaporated and the mixture was extracted with diethyl ether. After evaporation, silica gel chromatography (hexanes/Et_2O: 98/2; hexanes/Et_2O: 98/2, hexanes/Et_2O: 90/10, respectively) yielded the corresponding compounds **1a**−**c**.

***endo*-10-Fluoro-*exo*-10′-diphenylphosphanyltricyclo-[4.3.1.0^{1,6}]deca-1,3-diene (1a).** Yield: 70%. ^{1}H NMR (400 MHz, $CDCl_3$): δ 1.68 (m, 1H), 1.99 (m, 3H); 2.45 (m, 2H); 5.85 (dd, 2H, J = 11.5 Hz, J = 3.9 Hz), 6.05 (dd, 2H, J = 11.7 Hz, J = 3.9 Hz), 7.21 (m, 6H), 7.39 (m, 4H); ^{13}C NMR (101 MHz, $CDCl_3$): δ 133.7 (dd, J = 8.3 Hz, J = 5.2 Hz); 132.4 (d, J = 19.3 Hz); 127.7 (s); 127.4 (d, J = 6.7 Hz); 122.3 (s); 122.3 (d, J = 5.2 Hz); 73.6 (dd, J = 278.0 Hz, J = 44.4 Hz); 48.4 (dd, J = 10.3 Hz, J = 7.3 Hz); 34.5 (d, J = 13.9 Hz); 23.6 (d, J = 16.1 Hz). ^{31}P NMR (101 MHz, $CDCl_3$): δ −10.8 (d, J = 5.2 Hz). ^{19}F NMR (235 MHz, $CDCl_3$): δ −180.5 (d, J = 7.0 Hz). Exact mass for $C_{22}H_{20}FP$ (amu): Calcd: 334.128116; Found: 334.1291.

***endo*-10-Fluoro-*exo*-10′-thiophenyltricyclo[4.3.1.0^{1,6}]deca-1,3-diene (1b).** Yield: 58%. ^{1}H NMR (400 MHz, $CDCl_3$): δ 7.35(dm, 2H, J = 7.3 Hz); 7.22 (tm, 2H, J = 7.6 Hz); 7.15 (dm, 1H, J = 7.2 Hz); 6.09 (dd, 2H, J = 7.2 Hz, J = 2.6 Hz); 5.86 (dd, 2H, J = 7.1 Hz, J = 2.5 Hz); 2.09 (m, 2H); 1.85 (m, 2H); 1.69 (m, 1H); 1.58 (m, 1H). ^{13}C NMR (63 MHz, $CDCl_3$): δ 135.5 (d, J = 3.1 Hz); 129.5 (s); 128.0 (d, J = 1.7 Hz); 126.8 (s); 124.1 (d, J = 1.8 Hz); 121.6 (d, J = 3.7 Hz); 84.3 (d, J = 268.3 Hz); 50.0 (d, J = 12.6 Hz); 35.2 (s); 25.1 (d, J = 2.5 Hz). ^{19}F NMR (235 MHz, $CDCl_3$): δ −144.4. Exact mass for $C_{16}H_{15}FS$ (amu): Calcd: 258.087299; Found: 258.0865.

***endo*-10-Fluoro-*exo*-10′-trimethylsilyltricyclo[4.3.1.0^{1,6}]-deca-1,3-diene (1c).** Yield: 31%. ^{1}H (400 MHz, $CDCl_3$): δ 6.04 (dd, 2H, J = 7.1 Hz, J = 2.5 Hz); 5.82 (dd, 2H, J = 7.0 Hz, J = 2.6 Hz,); 2.05 (m, 2H); 1.89 (m, 2H); 1.56 (m, 1H); 1.35 (m, 1H); 0.22 (d, 9H, J = 1.0 Hz). ^{13}C NMR (63 MHz, $CDCl_3$): δ 122.5 (d, J = 2.2 Hz); 121.6 (d, J = 6.7 Hz); 69.3 (d, J = 237.8 Hz); 49.9 (d, J = 9.7 Hz); 35.4 (s); 27.6 (s);

−0.2 (d, $J = 3.8$ Hz). ^{19}F NMR (235 MHz, $CDCl_3$): δ −185.4. Exact mass for $C_{13}H_{19}FSi$ (amu): Calcd: 222.123456; Found: 222.1233.

Laser Flash Photolysis (LFP) Studies. For LFP studies, a stock solution of **1a**−**c** in the desired solvent was prepared to an optical density of 1.0−1.5 at 308 nm and placed in each cuvette (2 mL per cuvette) with various amounts of trapping agents. Suprasil quartz fluorescence free static cells and a special sample holder were used to avoid scattering of the laser beam. The LFP apparatus utilized a Lambda Physik LPX 100/200 excimer laser (308 nm, 150 mJ, 17 ns, XeCl excimer). Samples used in LFP experiments were deoxygenated by passing a flow of dry argon through the sample for 2 min. The analysis of the data was performed with the program IgorPro developed by Wavemetrics. Transient absorption spectra were obtained on an EG&G PARC 1460 optical multichannel analyzer fitted with an EG&G PARC 1304 pulse amplifier, an EG&G PARC 1024 UV detector, and a Jarrell-Ash 1234 grating. The monochromator used was an Oriel 77200. Signals were obtained with a photomultiplier tube detector and were digitalized by a Tektronix 5818A A/D transient digitizer. The spectrometer has been described elsewhere in detail.[5]

Protocols for Photolysis in Glassy Matrixes. A solution of **1a**−**c** in the desired solvent was prepared to an optical density of 1.0−1.5 at 300 nm and placed in each cuvette (3 mL per cuvette). Samples were deoxygenated by passing a flow of dry argon through the sample for 2 min. The cuvette was placed in a transparent quartz dewar and the temperature was cooled by the addition of liquid nitrogen. Photolysis was performed in a rayonet photochemical reactor using 300 nm UV lamps. The UV spectrum was recorded using a Perkin-Elmer lambda 6 UV/VIS spectrophotometer.

Density Functional Calculations. Geometries were fully optimized at the B3LYP level using the 6-31G(d) basis set, and harmonic frequencies were calculated at the same level. All the calculations were carried out with the Guassian98 software package.[6] Energies and zero-point vibrational energy (ZPVE) corrections were scaled by 0.9806 as noted.

III. Results

III.1. Fluorodiphenylphosphoryl Carbene (2a). We synthesized 10-chloro-10-fluorotricycloundecadiene as an endo/exo mixture at C-10 as shown in Scheme 1. *n*-Butyllithium undergoes metal−halogen exchange exclusively with the *exo*-chloride which was quenched with either diphenylphosphoryl chloride, phenylchlorosulfide, or trimethylsilylchloride to form **1a**−**1c**, respectively.

Transient and Glassy Matrix Spectroscopy. Laser flash photolysis (LFP) studies were performed using 308 nm pulses from a XeCl excimer laser. The transient spectra produced upon LFP of **1a** are given in Figure 1. All the transient spectra exhibit an average maximum absorbance around 330 nm. In the case of acetonitrile, a broad absorption band at higher wavelength (410 nm) is also observed. When excess oxygen is bubbled through the sample solution, the transient absorption at 330 nm is not modified, indicating that the carrier of this absorption is neither a radical, nor a triplet carbene nor a triplet excited state nor a triplet biradical.

Similar results were obtained upon photolysis (300 nm) of **1a** in glassy 3-methylpentane at 77 K. The data (Figure 2) show the growth of two absorption bands at 295 and 325 nm. After warming the sample to room temperature and re-cooling, the final spectrum (labeled RT) exhibits only a peak at 295 nm. Thus, the short wavelength band is due to a stable product that is generated during the photolysis. The 325 nm peak is associated with a reactive species

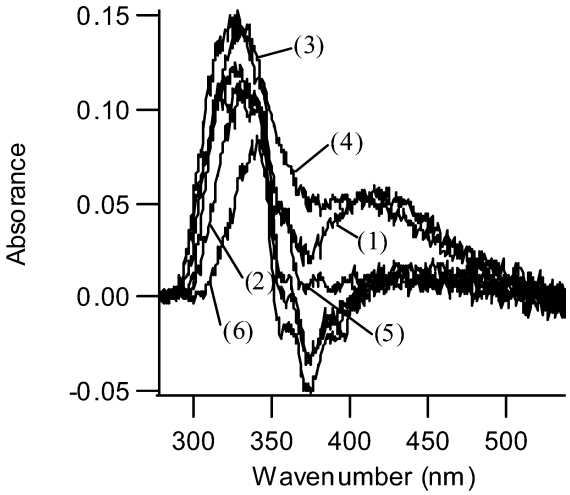

Figure 1. Transient UV spectrum produced by LFP (308 nm) of **1a** in several solvents. The spectrum was recorded immediately after the laser pulse over a window of 20 ns. (1) CH_3CN, (2) EtOAc, (3) C_6H_6, (4) CH_2Cl_2, (5) C_5H_{12}, (6) THF.

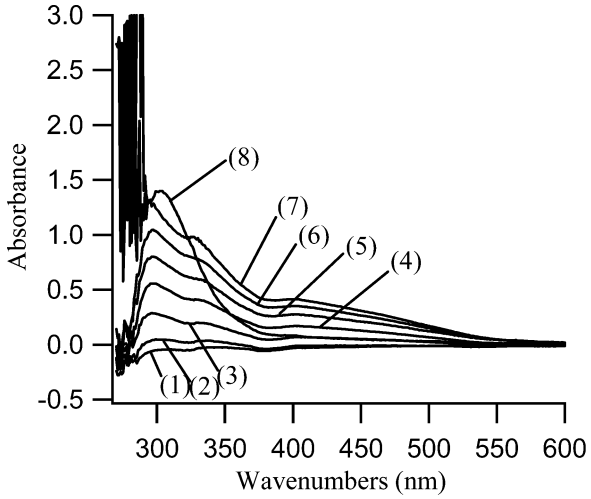

Figure 2. Differential UV spectrum produced by photolysis (300 nm) of **1a** at 77 K in 3-methylpentane. (1) 1 min, (2) 2 min, (3) 4 min, (4) 7 min, (5) 10 min, (6) 15 min, (7) 20 min, (8) after annealing to RT.

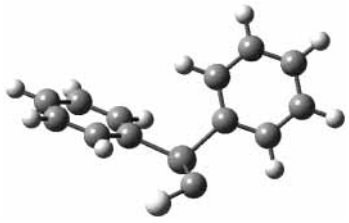

Figure 3. Results of DFT calculations (b3lyp/6−31 g(d)) on carbene **2a**. Selected calculated bond lengths and angles: d(FC) = 1.34 Å; d(CP) = 1.77 Å; FCP = 111.4 °. TD-DFT: 514.84 nm (f = 0.0040); 323.16 nm (f = 0.0486); 300.66 nm (f = 0.0341); 280.70 nm (f = 0.0032); 277.40 nm (f = 0.0164); 271.06 nm (f = 0.0223); 267.84 nm (f = 0.0096); 265.06 nm (f = 0.0153).

Density Functional Theoretical (DFT) Calculations. Density functional theoretical calculations on carbene **2a** were performed using the b3lyp/6−31 g(d) level of theory (Figure 3).[6] The predicted geometry of singlet **2a** reveals a bent carbene (the angle at the carbene center is 111.4°). Furthermore, the geometry

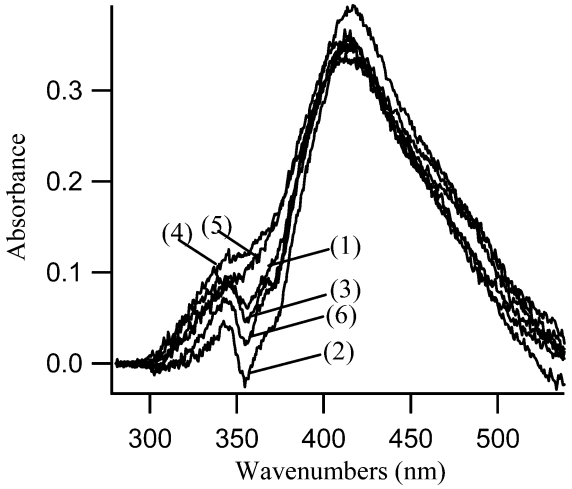

Figure 4. Transient UV spectrum produced by LFP (308 nm) of **1a** in the presence of pyridine in several solvents. The spectrum was recorded immediately after the laser pulse over a window of 20 ns. (1) CH_3CN, (2) EtOAc, (3) C_6H_6, (4) CH_2Cl_2, (5) pentane, (6) THF.

around the phosphorus atom is almost planar (the dihedral angle around the phosphorus atom of 34° and sum of the angles around it is 338°) which argues against $\sigma^3\lambda^3$ character of phosphorus. The PC bond length is calculated to be 1.77 Å. This value is intermediate between that of typical carbon−phosphorus single and double bond lengths[7] and is consistent with a $\sigma^3\lambda^4$ character of the phosphorus atom. These facts indicate that the lone pair on phosphorus is delocalized on the vacant orbital on the carbene center (a representation of the LUMO orbital is available in the Supporting Information and shows the corresponding interaction). Time-dependent density functional theory[8] with the same basis set predicts two strong vertical UV absorptions for carbene **2a** at 323 and 301 nm. Thus, the calculations suggest that the transient absorption at 325 nm observed by LFP and the carrier of the persistent species absorbing at the same wavelength in 3-methylpentane should be attributed to carbene **2a**.

Pyridine Ylides. Compound **1a** was studied by LFP in several solvents in the presence of pyridine (Figure 4). The formation of a pyridine ylide is observed in every case with a characteristic maximum absorbance at 414 nm.

The decay of transient absorbance at 330 nm was monitored along with the growth of absorbance at 414 nm in the presence of pyridine. Figure 5 demonstrates that there is an excellence correspondence of the dynamics at the two wavelengths. There is no doubt that the carrier of transient absorption of 325 nm reacts with pyridine to form a new compound that absorbs at 414 nm. At 414 nm, we can reasonably assume that the formation of the carbene−pyridine ylide **10** is observed. We therefore conclude that the signal observed at 330 nm is singlet carbene **2a**. We find that $k_{PYR} = 5 \times 10^8\ M^{-1}\ s^{-1}$, a value similar to that of other ground-state singlet carbenes.[9]

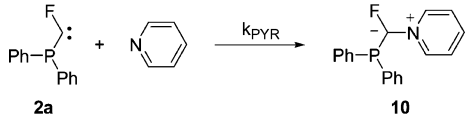

2a **10**

Solvent Effects on Carbene Lifetimes. The lifetimes of carbene **2a** in several solvents, monitored at 330 nm, are listed in Table 1. The carbene lifetime of 1 μs in cyclohexane is extended to 2 μs in cyclohexane-d_{12}. This indicates that the lifetime of **2a** is limited in part by insertion into C−H bonds of the solvent.

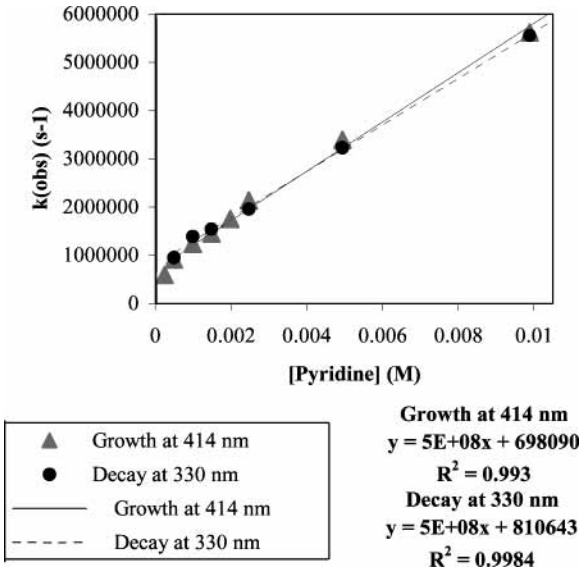

Figure 5. Plots of the observed rate constant of transient decay (330 nm) and absorption (414 nm) versus the concentration of pyridine produced by LFP (308 nm) of **1a** in cyclohexane.

TABLE 1: Rate Constants and Lifetime of Carbene 3A in Several Solvents

solvent	lifetime (μs)
cyclohexane	1.0
cyclohexane-d_{12}	2.0
pentane	1.2
acetonitrile	8.5
dichloromethane	9.8
benzene	7.2
tetrahydrofuran	8.5
valeronitrile	2.5

The magnitude of the isotope effect is consistent with that of other singlet carbenes.[10] When nonpolar solvents such as cyclohexane or pentane are employed, the lifetimes of the carbene are 1.0 and 1.2 μs, respectively.

One can intuitively predict that carbene **2a** will be strongly stabilized due to the interaction of the lone pair on the phosphorus atom with the vacant orbital of the carbene carbon atom, resulting in the mesomeric structure shown below. TD-DFT calculations are consistent with this hypothesis. As mentioned previously, the calculated C−P bond length is shorter than that expected for a normal C−P single bond. Furthermore, a Natural Population Analysis[11] was performed. This analysis indicates that the phosphorus atom has a net positive charge of +0.90 consistent with its $\sigma^3\lambda^4$ character. There is corresponding negative charge on the carbene center (−0.03), fluorine atom (−0.33) and the two ipso carbon atoms (−0.38 and −0.36), justifying the mesomeric structure below.

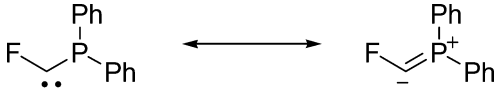

2a

We hypothesized that this delocalization and the resulting charge separation might lead to strong interactions of the carbene with solvent. Indeed, when more polar solvents are used (such as acetonitrile, dichloromethane, and THF), the carbene lifetime is lengthened by a factor of ≈10. One can speculate that the carbene center is stabilized either by the polarity of the solvent, or by some stronger solvent−carbene interaction.

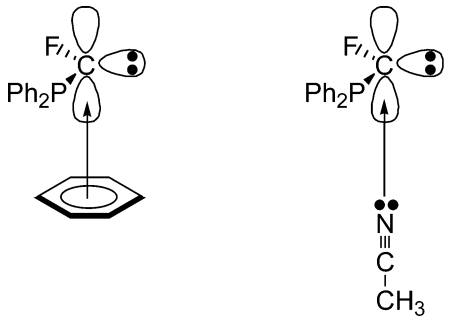

When benzene is employed, the observed lifetime of the carbene is 7.2 μs. Small amounts of THF and benzene in cyclohexane do not increase the lifetime, suggesting that there is no stabilization of the carbene by specific solvation as shown above.

Calculated Carbene−Acetonitrile Complexes. To better understand the solvent effects on the lifetime of carbene **2a**, we performed DFT calculations on the hypothetical complex between carbene **2a** and acetonitrile at the b3lyp/6−31 g(d) level of theory. In these calculations, the bond length between the carbenic carbon and the acetonitrile nitrogen atom was fixed between 1.4 and 4.4 Å and the structures were optimized. These structures do not correspond to stationary points, but were used in the construction of a Morse potential. The results are presented in Figures 6 and 7. The two widely separated molecules (**2a** and acetonitrile) were chosen as the reference energies. At 5.03 Å, we predict the formation of a weak hydrogen-bonded complex. No evidence was obtained for the formation of a π complex between the lone pair of electrons on nitrogen and the carbene center.

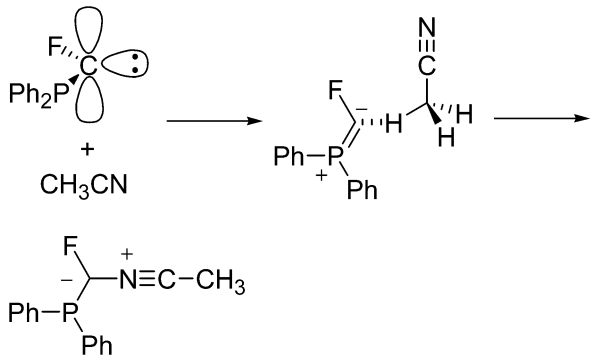

11

DFT calculations predict there will be a substantial barrier of 10.43 kcal/mol to forming ylide **11**. We propose that this process requires the rotation of the acetonitrile molecule resulting in the breaking of the calculated C−H bonding interaction and the loss of stabilization due to the interaction

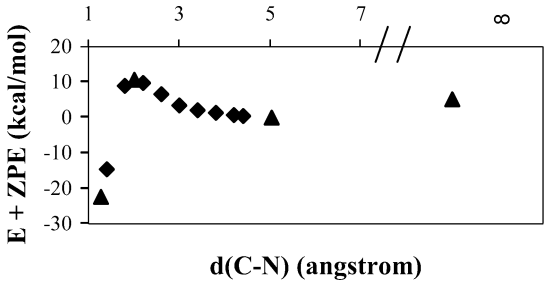

Figure 6. Calculated energy changes (b3lyp/6−31 g(d)) during the approach of one molecule of acetonitrile to carbene **2a**.

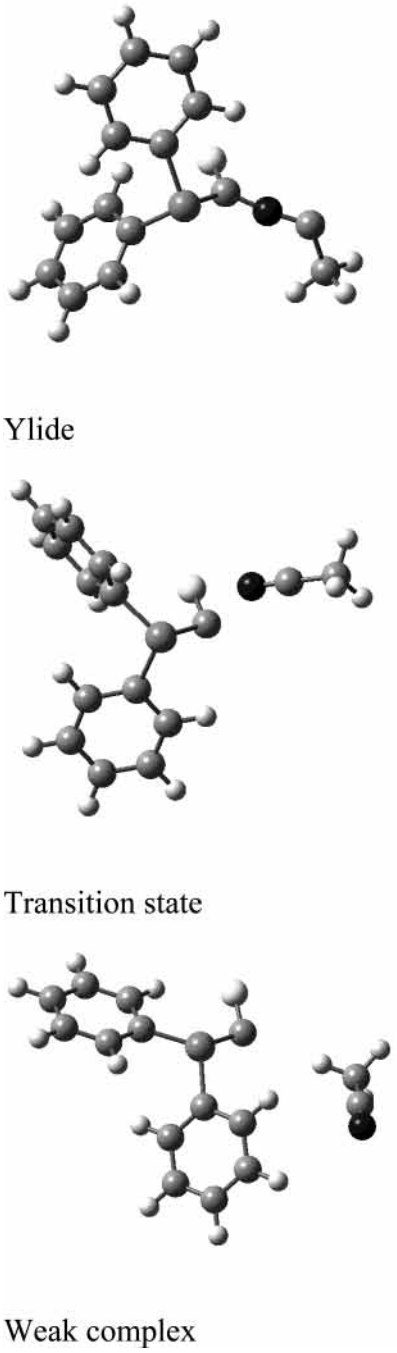

Figure 7. Calculated geometries (b3lyp/6−31 g(d) during the approach of an acetonitrile molecule to carbene **2a** with nitrile−ylide formation: ylide (d = 1.273 Å), transition state (d = 2.011 Å), and weak complex (d = 5.030 Å).

of the phosphorus lone pair and the carbene vacant orbital. Thus, ylide formation with carbene **2a** is predicted to be a slow process relative to other carbene reactions.

As mentioned previously, LFP of diene **1a** in acetonitrile produces a long wavelength absorption band at 410 nm. Unfortunately, its intensity is low and we were not able to resolve the kinetics of its formation at this specific wavelength. TD-DFT calculations predict that ylide **11** will have vertical absorption bands below 360 nm with a maximum absorbance at 306 and 289 nm. On the basis of this computational evidence, we suggest that the carrier of the 410 nm band is not ylide **11** and, at this time, this transient species is not identified.

*Calculated Singlet−Triplet Energy Separation of **2a**.* The relative energies of the singlet and triplet states of fluorodiphen-

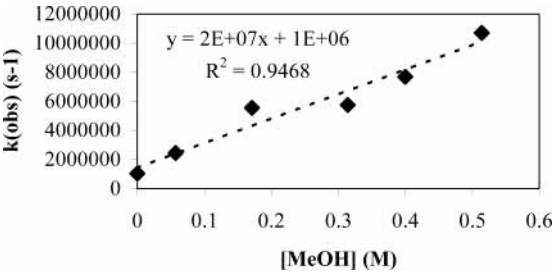

Figure 8. A plot of the observed rate constant of transient decay (330 nm) versus the concentration of methanol produced by LFP (308 nm) of **1a** in cyclohexane.

TABLE 2: Calculated Relative Energies (kcal/mol, scaled, b3lyp/6−31 g(d)) of the Singlet and Triplet States of Carbene 2a in Several Solvents and in the Gas Phase (The singlet is predicted to be the ground state in the gas phase and in all solvents examined.)

	E (singlet)	*E* (triplet)	Δ*E*(S/T)
gas phase	0	9.905	9.905
c-hexane	−1.498	8.785	10.283
benzene	−1.616	8.647	10.263
THF	−3.413	7.359	10.771
dichloromethane	−3.713	7.260	10.973
acetonitrile	−4.376	6.807	11.182

ylphosphorylcarbene were computed using DFT methods with the b3lyp/6−31 g(d) basis set.

As expected for a halocarbene, the singlet is predicted to be the ground state in the gas phase (the singlet/triplet gap $\Delta E_{S/T}$ = 9.9 kcal/mol). This level of theory is known to overestimate the stability of triplet carbenes relative to singlet carbenes.[12] In the case of methylene (CH_2) this level of theory predicts a singlet−triplet energy separation of 13 kcal/mol even though the experimental value is 9.05 kcal/mol.

The singlet carbene has a calculated dipole moment of 3.6770 D, the triplet carbene dipole moment is predicted to be 2.4388 D. Thus, these calculations were repeated in a solvent force-field using the Polarized Continuum Model of Tomasi et al.[12] The results are given in Table 2. Polar solvents are found to differentially stabilize the singlet carbene although the effect is rather small. $\Delta E_{S/T}$ increases from 10.3 kcal/mol in cyclohexane to 11.2 kcal/mol in acetonitrile showing that polar solvents better stabilize the singlet than the triplet state. Hadad and co-workers have reported related findings with arylcarbenes.[14]

*Bimolecular Reactions of **2a**.* Specific solvation is often manifested as a retardation of the rate of bimolecular chemical reactions.[15] As shown in Figure 8, methanol accelerates the rate of decay of fluorodiphenylphosphorylcarbene in cyclohexane. A plot of k_{OBS} versus [methanol] is linear with $k_{CH_3OH} = 2 \times 10^7$ M^{-1} s^{-1} in cyclohexane. The absolute rate constants of reaction of **2a** with methyl acrylate (Figure 9) and tetramethylethylene (Figure 10) were determined in cyclohexane, acetonitrile, and benzene. The results are collected in Table 3. It is clear that the cycloaddition reaction rate constants of **2a** show little variation with solvent. Thus, there is no kinetic evidence of specific solvation of fluorodiphenylphosphorylcarbene **2a**.

III.2. Fluorothiophenylcarbene (2b). DFT calculations (b31yp/6−318/d) were performed on carbene **2b** in its singlet state. The geometry of fluorothiophenylcarbene and key parameters are given in Figure 11 along with the UV−Vis spectrum of **2b** predicted by TD-DFT calculations. According to the TD-DFT calculations, the sulfur-substituted carbene **2b** will not absorb significantly above 300 nm and will be more difficult to observe directly by transient UV−Vis spectroscopy than the phosphorus analogue **2a**.

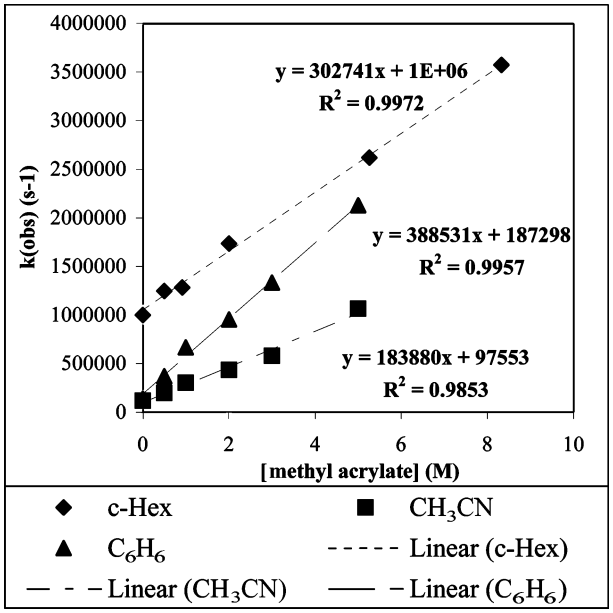

Figure 9. Plots of the observed rate constant of transient decay (330 nm) versus the concentration of methyl acrylate produced by LFP (308 nm) of **1a** in several solvents.

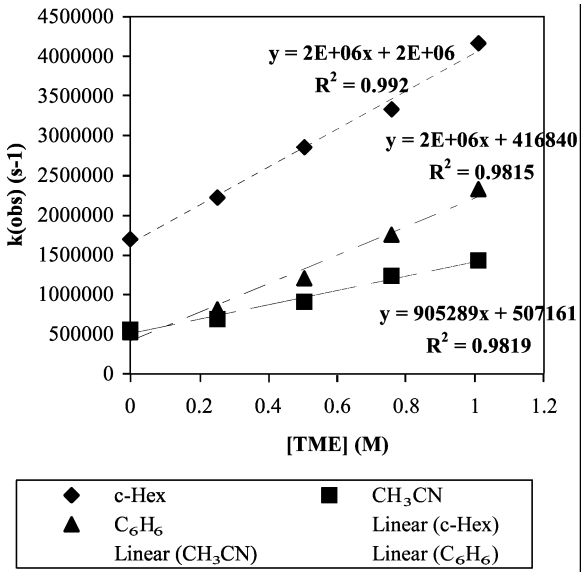

Figure 10. Plots of the observed rate constant of transient growth (414 nm) versus the concentration of tetramethylethylene produced by LFP (308 nm) of **1a** in several solvents containing 1.978 mM of pyridine.

TABLE 3: Absolute Rate Constants of Reaction of Carbene 2A with Alkenes Measured in Several Solvents

solvent	*k* (methyl acrylate) (M^{-1} s^{-1})
cyclohexane	3.0×10^5
benzene	3.9×10^5
CH_3CN	1.8×10^5

solvent	*k* (TME) (M^{-1} s^{-1})
cyclohexane	2.0×10^6
benzene	2.0×10^6
CH_3CN	9.0×10^5

LFP of **1b** (308 nm) produced transient spectra as a function of solvent (Figure 12). A maximum transient absorption at 360 nm was observed in every solvent. The carrier of this transient absorption was shown to react rapidly with oxygen ($\tau(N_2)/\tau(O_2)$ = 19 in pentane), in contrast to phosphoryl carbene **2a**, whose lifetime is not appreciably influenced by oxygen.

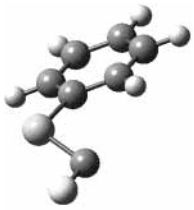

Figure 11. Results of DFT calculations on carbene **2b** (b3lyp/6−31 g(d)). Selected calculated bond lengths and angles: d(FC) = 1.336 Å; d(CS) = 1.75 Å; FCS = 105.3 °. TD-DFT: 394.16 nm (f = 0.0045); 288.77 nm (f = 0.0508); 272.09 nm (f = 0.0072); 240.51 nm (f = 0.0351); 235.31 nm (f = 0.0025); 226.90 nm (f = 0.0124); 215.34 nm (f = 0.0245); 212.11 nm (f = 0.0960).

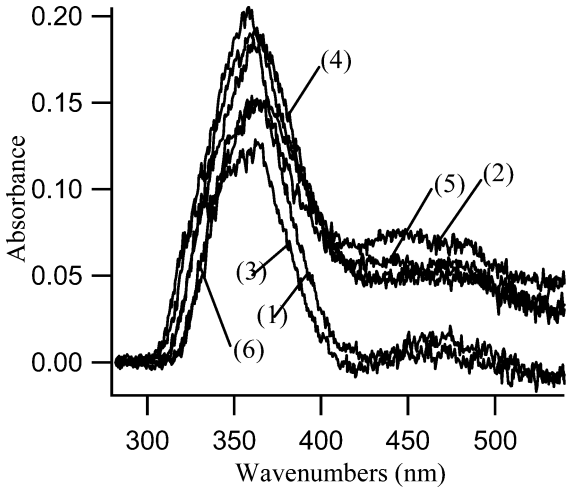

Figure 12. Transient UV spectrum produced by LFP (308 nm) of **1b**. The spectrum was recorded immediately after the laser pulse over a window of 20 ns. (1) CH_3CN, (2) EtOAc, (3) C_6H_6, (4) CH_2Cl_2, (5) C_5H_{12}, (6) THF.

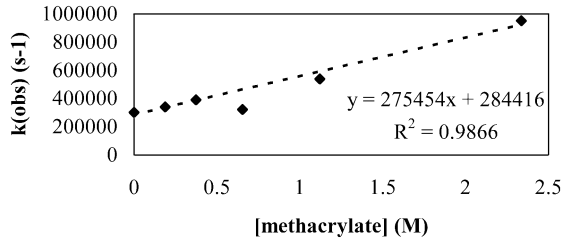

Figure 13. A plot of the observed rate constant of transient decay (360 nm) versus the concentration of methyl methacrylate produced by LFP (308 nm) of **1b** in cyclohexane.

The transient obtained by LFP of **1b** reacts with methyl methacrylate. A plot (Figure 13) of $1/\tau$ versus [alkene] is linear with a slope of 2.8×10^5 M^{-1} s^{-1} in cyclohexane at ambient temperature.

LFP of **1b** in several pyridine-containing solvents produces the transient spectra shown in Figure 14. The carrier of the broad intense pyridine-dependent transient at 406 nm is assigned to ylide **12** by analogy to the behavior of **2a**.

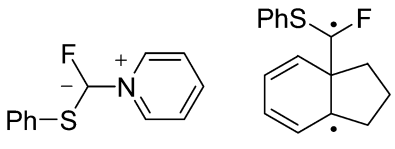

12

13

A plot of k_{OBS} to the formation of ylide **12** versus [pyridine] is linear (Figure 15) with slope $k_{pyr} = 2.0 \times 10^7$ M^{-1} s^{-1}. The

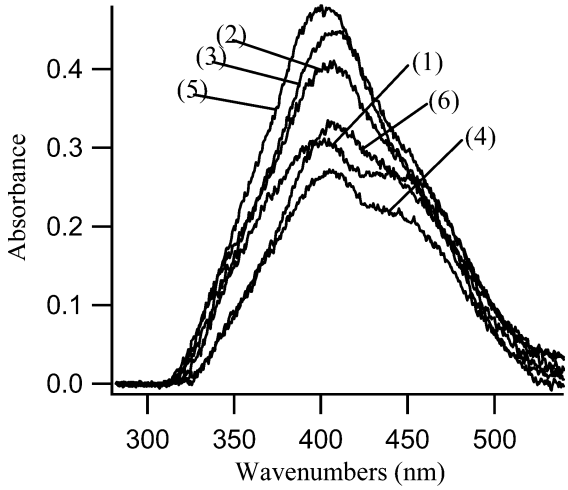

Figure 14. Transient UV spectrum produced by LFP (308 nm) of **1b** in the presence of pyridine. The spectrum was recorded immediately after the laser pulse over a window of 20 ns. (1) CH_3CN, (2) EtOAc, (3) C_6H_6, (4) CH_2Cl_2, (5) C_5H_{12}, (6) THF.

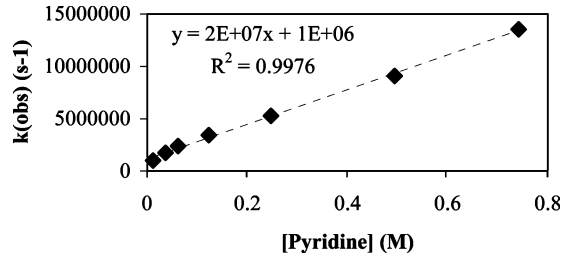

Figure 15. A plot of the observed rate constant of transient decay (406 nm) versus the concentration of pyridine produced by LFP (308 nm) of **1b** in cyclohexane.

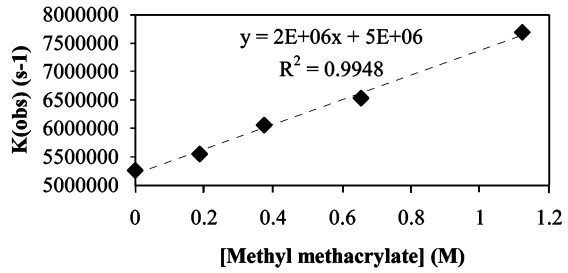

Figure 16. A plot of the observed rate constant of transient decay (406 nm) versus the concentration of methyl methacrylate produced by LFP (308 nm) of **1b** in cyclohexane containing 0.247 M of pyridine.

intercept of the plot ($1/\tau$) indicates that the carbene lifetime in cyclohexane is 1 μs. A plot of k_{OBS} versus [methyl methacrylate] at a constant pyridine concentration of 0.247 M is given in Figure 16. The slope of this plot is the absolute rate constant of reaction of carbene **2b** with methyl methacrylate, and is 2.0×10^6 M^{-1} s^{-1}.

The data obtained by the pyridine ylide probe method is in poor agreement with the data obtained by direct observation of the effect of methyl methacrylate on the rate of decay of the transient absorbing at 360 nm, produced by LFP of **1b** in the absence of pyridine. Furthermore, we found that the yield of pyridine ylide is unaffected by the presence of oxygen in the solution (as expected for the reaction of a singlet carbene). We conclude, therefore, that the oxygen-sensitive carrier of the transient absorption at 360 nm is not carbene **2b**.

We speculate that the carrier of transient absorption at 360 nm is triplet biradical **13**, derived from one-bond cleavage of precursor **1b**, in competition with two-bond cleavage to form

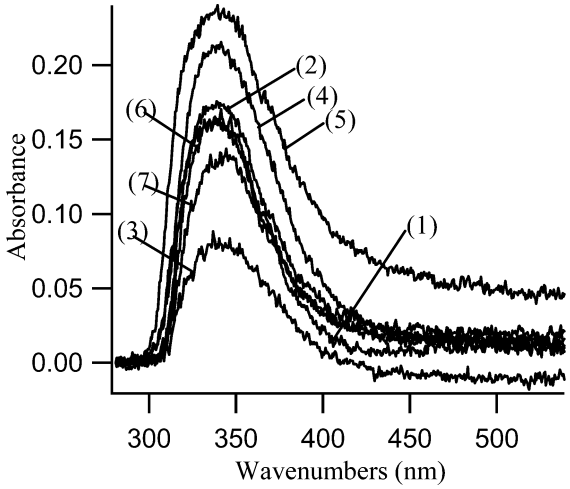

Figure 17. Transient UV spectrum produced by LFP (308 nm) of **1c**. The spectrum was recorded immediately after the laser pulse over a window of 20 ns. (1) AcOEt, (2) C_6H_6, (3) CCl_4, (4) CH_2Cl_2, (5) CH_3CN, (6) C_5H_{12}, (7) THF.

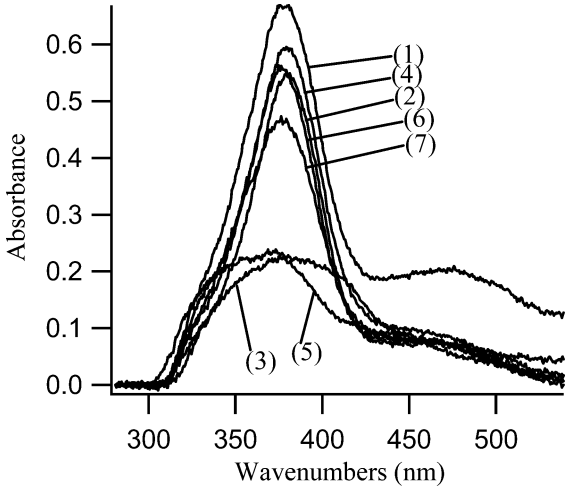

Figure 18. Transient UV spectrum produced by LFP (308 nm) of **1c** in the presence of pyridine. The spectrum was recorded immediately after the laser pulse over a window of 20 ns. (1) AcOEt, (2) C_6H_6, (3) CCl_4, (4) CH_2Cl_2, (5) CH_3CN, (6) C_5H_{12}, (7) THF.

TABLE 4: Relative Energies and TD-DFT Calculations on Several Possible Intermediates at B3Lyp/6−31 g(d)

13
E + ZPE (scaled)= 0 kcal/mol TD-DFT: 449 (f = 0.0007); 416 (f = 0.0019); 360 (f = 0.0014);355 (f = 0.0042); 343 (f = 0.036); 336 (f = 0.0073); 331 (f = 0.0071); 319 (f = 0.057)
indan + 2b
E + ZPE (scaled)= −17.8 kcal/mol TD-DFT: **Indan**: 233 (f = 0.0178); 206 (f = 0.0082); 179 (f = 0.3698); 178 (f = 0.6898) TD-DFT: **3b**: 394 (f = 0.0045); 289 (f = 0.0508); 272 (f = 0.0072); 240 (f = 0.0351)

carbene **2b** and indan. Such intermediates, although never observed, were postulated to explain the photochemical isomerization of certain cyclopropanes.[16]

The energies of indan plus **2b** and triplet **13** are given in Table 4 along with the calculated (TD-DFT) UV−Vis spectrum of triplet biradical **13**. The TD-DFT calculations predict that, unlike carbene **2b**, triplet biradical **13** will absorb strongly between 300 and 350 nm, the active region observed upon LFP of **1b** in the absence of pyridine. This assignment explains the

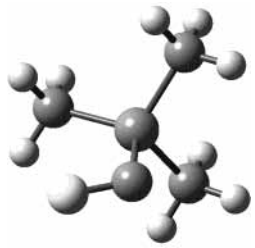

Figure 19. Results of DFT calculations (b3lyp/6−31 g(d)) on carbene **2c**. Selected calculated bond lengths and angles: d(FC) = 1.335 Å; d(CSi) = 1.950 Å; FCS = 109.1 °. TD-DFT: 1120.79 nm (f = 0.0002); 247.39 nm (f = 0.0144); 234.16 nm (f = 0.0345); 206.61 nm (f = 0.0714); 194.74 nm (f = 0.0122); 184.73 nm (f = 0.0200); 176.80 nm (f = 0.0223); 175.23 nm (f = 0.0754).

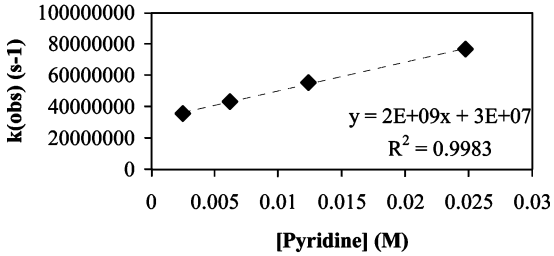

Figure 20. A plot of the observed rate constant of transient decay (380 nm) versus concentration of pyridine produced by LFP (308 nm) of **1c** in carbon tetrachloride.

sensitivity of the transient toward oxygen and its reactivity toward methyl methacrylate. It is possible that the photolysis of diene **1a** produces both phosphorus carbene **2a** and a biradical analogue **13**. However, since carbene **1a** absorbs strongly between 300 and 350 nm, it is possible that the transient spectrum of such a biradical is masked.

III.3. Fluorotrimethylsilylcarbene (2c). LFP (308 nm) of **1c** produces the transient spectra of Figure 17. The transient lifetime monitored at 340 nm is 1 μs. The lifetime of the transient is not sensitive to oxygen ($k(N_2)/k(O_2)$ = 0.99 in pentane).

LFP (308 nm) of **1c** in several pyridine-containing solvents produces the transient spectra presented in Figure 18. The transient absorption is attributed to ylide **14**.

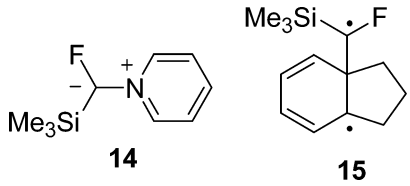

14 **15**

The yield of ylide **14** is slightly sensitive to the presence of oxygen ($Abs_{max}(N_2)/Abs_{max}(O_2)$ = 1.25 in pentane). DFT calculations of carbene **2c** (Figure 19) and TD-DFT calculations predict that **2c** has no significant absorption above 250 nm. This is evidence that the transient detected at 340 nm in the absence of pyridine is not carbene **2c**.

A plot of the observed rate constant of formation of ylide **14** versus [pyridine] is given in Figure 20. The slope of this plot is $k_{PYR} = 2 \times 10^9$ M^{-1} s^{-1}. The intercept of this plot indicates that the lifetime of carbene **2c** is 33 ns in carbon tetrachloride in the absence of pyridine.

TD-DFT calculations (b3lyp/6−31 g(d)) predict that diradical intermediate **15** has vertical absorption bands at 271, 288, 320, and 339 nm. The latter value is consistent with the observed value of 340 nm. Indeed, photolysis ($CF_2ClCFCl_2$, 300 nm) of **1c** leads to the formation of a stable isomeric photoproduct

detected by GC-MS in low yields. It is tempting to assign the transient signal absorbing at 340 nm to biradical **15**, which forms the product of epimerization of **1c**. However, the oxygen independence of the transient lifetime does not appear to be consistent with the presence of a biradical intermediate. Therefore, the identity of the transient observed upon LFP of **1c** cannot be assigned with confidence at this time

IV. Conclusion

Laser flash photolysis (LFP, 308 nm) of *endo*-10-fluoro-*exo*-10-substituted tricyclo[4.3.1.0]-decadienes produces indan and singlet fluorocarbenes substituted with diphenylphosphoryl, phenylsulfanyl, and trimethylsilyl groups. All three carbenes react with pyridine to form UV−Vis active ylides. The ylides are formed exponentially with observed rate constants of k_{OBS}. Plots of k_{OBS} versus [pyridine] are linear with slopes equal to the absolute rate constant of reaction of carbene with pyridine of $k_{PYR} = 5 \times 10^8\ M^{-1}\ s^{-1}$ (fluorodiphenylphosphorylcarbene), $k_{PYR} = 2 \times 10^7\ M^{-1}\ s^{-1}$ (fluorophenylsulfanylcarbene) and $k_{PYR} = 2 \times 10^9\ M^{-1}\ s^{-1}$ (fluorotrimethylsilylcarbene). Fluorodiphenylphosphorylcarbene can also be detected directly through absorption at 325 nm. Its lifetime and reactivity are slightly modulated by solvent.

Acknowledgment. Support of this work by the National Science Foundation, a GAANN Fellowship of the Department of Education (E.M.T.) and the Ohio Supercomputer Center is gratefully acknowledged.

Supporting Information Available: Optimized geometries, energies, zero-point and thermal corrections and IR frequencies for compounds **2a**−**c**, **13**, **15,** and compounds presented in Figure 7. This material is available free of charge via the Internet at http://pubs.acs.org.

References and Notes

(1) Hartwig, J. F.; Jones, M., Jr.; Moss, R. A.; Lawrynowicz, W. *Tetrahedron Lett.* **1986**, *27*, 5907−5910.

(2) Likhotvorik, I.; Zhu, Z.; Tae, E. L.; Tippmann, E.; Hill, B. T.; Platz, M. S. *J. Am. Chem. Soc.*, **2001**, *123*, 6061.

(3) Birch, A. J.; Walkerk, A. M. *Aust. J. Chem.* **1971**, *24*, 513.

(4) Dolbier, W. R.; Burkholder, C. R. *J. Org. Chem.* **1990**, *55*, 589.

(5) Martin, C.B.; Shi, X.; Tsao, M.-L.; Karweik, D.; Brooke, J.; Hadad, C. M.; Platz, M. *J. Phys. Chem. B* **2002**, *106*, 10263.

(6) (a) Becke, A. D. *J. Chem. Phys.* **1993**, *98*, 5648. (b) Lee, C.; Yang, W.; Parr, R. G. *Phys. Rev. B* **1998**, *37*, 785. (c) Frisch, M. J.; Trucks, G. W.; Schlegel, H. B.; Scuseria, G. E.; Robb, M. A.; Cheeseman, J. R.; Zakrzewski, V. G.; Montgomery, J. A., Jr.; Stratmann, R. E.; Burant, J. C.; Dapprich, S.; Millam, J. M.; Daniels, A. D.; Kudin, K. N.; Strain, M. C.; Farkas, O.; Tomasi, J.; Barone, V.; Cossi, M.; Cammi, R.; Mennucci, B.; Pomelli, C.; Adamo, C.; Clifford, S.; Ochterski, J.; Petersson, G. A.; Ayala, P. Y.; Cui, Q.; Morokuma, K.; Malick, D. K.; Rabuck, A. D.; Raghavachari, K.; Foresman, J. B.; Cioslowski, J.; Ortiz, J. V.; Baboul, A. G.; Stefanov, J. V.; Liu, G.; Liashenko, A.; Piskorz, P.; Komaromi, I.; Gomperts, R.; Martin, R. L.; Fox, D. J.; Keith, T.; Al-Laham, M. A.; Peng, C. Y.; Nanayakkara, A.; Gonzalez, C.; Challacombe, M.; Gill, P. M. W.; Johnson, B.; Chen, W.; Wong, M. W.; Andres, J. L.; Gonzalez, C.; Head-Gordon, M.; Replogle, E. S.; Pople, J. A. *Gaussian 98*, Revision A.7; Gaussian, Inc.: Pittsburgh, PA, 1998.

(7) Corbridge, D. E. C. *Phosphorus: An outline of its chemistry, biochemistry and technology* (5th ed.); Elsevier: Amsterdam, 1995; p 54.

(8) Casida, M. E.; Jamorski, C.; Casida, K. C.; Salahub, D. R. *J. Chem. Phys.* **1998**, *108*, 4439.

(9) (a) Bucher, G.; Scaiano, J. C.; Platz, M. S. *Kinetics of Carbene Reactions in Solution*; Landolt-Bornstein, Group II, Volume 18, Subvolume E2; Springer: Berlin, Germany, 1998; p 141. (b) Ge, C.-S.; Jang, E. G.; Jefferson, E. A.; Liu, W.; Moss, R. A.; Wlostowska, J.; Xue, S. *Chem. Commun.* **1994**, 1479.

(10) Admasu, A.; Gudmundsdöttir, A. D.; Platz, M. S. *J. Phys. Chem.* **1997**, *101*, 3832.

(11) Reed, A. E.; Weinhold, F. A.; Curtiss, C. A. *Chem. Rev.* **1988**, *88*, 899.

(12) Scott, A. P.; Platz, M. S.; Radom, L. *J. Am. Chem. Soc.* **2001**, *123*, 6069.

(13) Tomasi, J.; Persico, M. *Chem. Rev.* **1994**, *94*, 2027.

(14) (a) Wang, Y.; Hadad, C. M.; Toscano, J. P. *J. Am. Chem. Soc.* **2002**, *124*, 1761. (b) Geise, G. M.; Wang, Y.; Mykhaylova, O.; Frink, B.T.; Toscano, J. P.; Hadad, C. M. *J. Org. Chem.* **2002**, *67*, 3079.

(15) Heyding, R. D.; Winkler, C. A. *Can. J. Chem.* **1951**, *29*, 790.

(16) (a) Engle, P. S.; Bodager, G. A. *J. Org. Chem.* **1986**, *51*, 4792. (b) Buchwalter, S. L. *Tetrahedron* **1984**, *40*, 5097.